AD-A180 306 THEORY OF ELECTRONIC STATES AND FORMATION ENERGIES OF DEFECT COMPLEXES IN..(U) ARIZONA STATE UNIV TEMPE DEPT OF PHYSICS O F SANKEY AUG 86 N00014-85-C-0442 1/1

UNCLASSIFIED F/G 20/12 NL

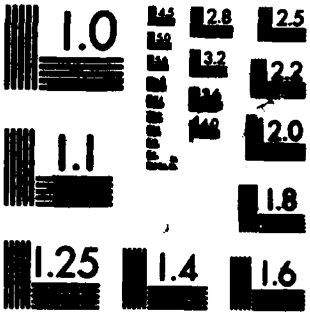

MICROCOPY RESOLUTION TEST CHART
NATIONAL BUREAU OF STANDARDS-1963-A

Arizona State University, Department
of Physics, Tempe, AZ 85287

DTIC FILE COPY (12)

Annual letter report by O. F. Sankey, P.I. for N00014-85-0442.

Theory of electronic states and formation energies of defect complexes, interstitial defects and crystal growth in semiconductors.

Period covering August 1985 - August 1986.

AD-A180 306

~~We believe~~ significant progress has been acheived on a number of areas described in our proposal. We have (1) successfully developed and applied a theory to understand the deep to shallow transition of the bandgap energy levels of large chalcogen complexes in Si silicon, (2) have developed an ab-initio tight-binding-like electronic structure method for solids, (3) have made great progress in understanding the energetics of interstitial impurities in compound semiconductors, (4) have developed a theory to predict equilibrium concentrations of intrinsic and extrinsic defects in semiconductors, (5) have performed the first molecular dynamics simulations of a compound semiconductor surface, and (6) have studied the hydrogen halide molecular crystals under pressure. A brief summary of these topics will now be given.

A theory for the bandgap levels of large defect complexes has been developed and applied to large (up to five atoms) chalcogen S, Se, or Te complexes in Si. It is found that the number of bandgap levels is equal to the number of impurities in the cluster. Most of these levels are however electrically inert, except for the the upper pair of levels. We find that the wavefunction character for these "active" levels is very different to that of the isolated impurity. The theory predicts that the "active" uppermost level continuously changes from being deep-level-like to more effective-mass-like as the size of the defect complex increases. A number of intra-center transitions between localized bound states have been predicted. The theory explains many of the experimental findings on these systems. The bandgap levels for a complex of one to five chalcogen impurities is shown in Fig. 1.

DISTRIBUTION STATEMENT A
Approved for public release;
Distribution Unlimited

(1)

87 4 7 003

We have developed a new method for the efficient calculation of the electronic structure in solids. Our method is highly physical and uses a linear combination of pseudoatomic orbitals in the first-principles local density pseudopotential approximation. We have used this method to investigate such basic properties as lattice constant, bulk modulus, vibrational mode frequencies, band structures and charge densitites in ten different semiconducting materials of technological importance. We have found that this tight-binding-like technique gives exellent results when compared to the more rigorous plane wave expansion method. Some results are shown in Fig. 2.

We have used the technique described above to study the formation energy and near bandgap levels of interstitial impuritites in IV-IV, III-V, and II-VI semiconductors. We have discovered an interesting interplay between interstitial site preference and bandgap levels which causes (in some circumstances) the impurity to switch from one interstitial site to another as the fermi-level is changed. These findings may have importance in understanding diffusion processes in compound semiconductors, and in determining the predominant native defects. The physics describing this interplay between the two interstitial sites (which we refer to as T_A and T_C) is shown in Fig. 3. Near bandgap interstitial levels for a number of defects in GaAs and ZnSe are shown in Fig. 4

These calculations have led us to work on predicting, entirely from first principles, the equilibrium concentrations of a variety of defects in semiconductors including native defects such as antisites, vacancies, and interstitials. This exciting area is being pursued presently.

The type of calculations we are presently using are very similar in spirit to those of the tight-binding approximation used in a wide variety of applications in semiconductors. Our technique however, is totally ab-initio and requires no fitting to experiment and has no adjustable parameters. This makes it ideal for the study of systems where little is known experimentally.

Using an *empirical* tight-binding method (which does require fitting to experiment), we have also performed the first molecular dynamics simulation of a compound semiconductor surface using Hellmann-Feynman forces. The calculations use a parameterized form of the electron ion interaction, but have the advantage of being relatively simple to perform. A unique feature of these calculations is that they include the forces generated by the microscopic electronic states and include a number of many body effects. Eventually we would like to meld this type of molecular dynamics simulation with the above ab-initio "tight-binding" technique. The relaxation angle θ for the (110) surface derived from such a simulation are shown in Fig. 5. These results are obtained by following the motion of the atoms in time when a fictitious damping is introduced so that the atoms approach their eqiulibrium configuration.

We have also worked on a class of unusual molecular solid, the hydrogen halides HF, HCl and HBr. These materials are lattice dynamically non-linear, and we have investigated these materials theoretically and have studied their pressure dependence.

Fig. 1.

Theoretical curves of the energy levels (in the gap between Ev and Ec) for "tetrahedral" nearest-neighbor substitutional clusters of from one to five chalcogen (S, Se, or Te) impuritites in Si. The central atom in the cluster was chosen to be S and there are n (n= 2, 3, 4, or 5) impurity atoms in the defect cluster around the central atom. We fix the potential of the central atom Vs(1) to that of sulfur, and vary the defect potentials Vs(x) of the other (one to four) atoms simultaneously. The impurity potential Vs(x) is negative for atoms more electronegative than the host Si atom, and positive for more electropositititve impurities. It is zero when the n "defects" surrounding the central sulfur impurity are host Si atoms -- in this case the only level in the gap is that due to the isolated sulfur defect. The energy level of the isolated sulfur impurity, S_1^0, is driven down toward the valence band when it is clustered with other electronegative atoms. Other states are also formed due to the clustering. The uppermost levels of sulfur cluster complexes of 2 to 5 atoms are shown explicitly at the defect potential of about -5eV appropriate to sulfur. Note the upward trend toward the conduction band of the highest levels indicating a continuous transition from "deep" to "shallow-like" behavior as the cluster size increases from 2 to 5 defects.

Fig. 2.

(a) The transverse optic mode frequency computed entirely from first principles using an sp^3d^5 pseudoatomic orbitals in a tight-binding-like hamiltonian, compared to experimental values. The trends in these ten materials are predicted perfectly, and the agreement with experiment on an absolute scale is excellent.

(b) Comparison of the predicted lattice constants of semiconducting materials using sp^3d^5 pseudoatomic orbitals with experiment.

(c) Same as (b) but for bulk modulus. These results show that the technique is accurate enough to be useful in a variety of electronic structure/total energy calculations, and are easy to implement. The technique is only slightly less accurate than the more conventional, but more rigorous, planewave expansion techniques.

Fig. 3.

(a) The geometry of the tetrahedral interstitial site, labeled I, in a compound semiconductor. The interstitial is surrounded by four nearest neighbors labeled 1 through 4. Two such sites exist; the T_A and T_C interstitial sites. The T_A (T_C) site has a nearest-neighbor environment of four anions (cations). One site ought to be preferred over the other for a specific impurity.

(b) A simple schematic three level diagram for an interstitial (chosen to be Zn in GaAs for discussion) at the T_A (right panel) and T_C (left panel) tetrahedral sites. The Zn s-orbitals interacts with the valence and conduction bands with different strengths due to the different environments. The single dashed line indicates a weak interaction, while the double dashed line a strong interaction. The Zn s-orbital pushes down on the valence level and up on the conduction level. The circles indicate electrons and the diagram indicates the Zn^0 center. Note that the Zn related "deep" level is always lower in energy at the T_C-site than at the T_A-site, but that the change in energy of the valence bands favors the T_A-site. These two energy terms are competitive, and the lowest energy configuration is expected to depend on the occupancy of the deep level.

(c) The total energy for the T_A and T_C sites of interstitial Zn in GaAs as a function of the chemical potential in the gap. Note that the bandgap deep energy levels (indicated by short vertical lines) are lower in energy at the T_C-site than the T_A. Also note that when the deep levels are empty (+2 charge state), the system prefers the T_A-interstitial site, but that the T_A and T_C sites are nearly degenerate in energy when the deep levels are occupied. These features are in agreement with the qualitative physics of the diagram in (b).

Fig. 4.

(a) Bandgap energy levels for interstitial impurities in GaAs at the two tetrahedral interstitial sites (T_A and T_C). A number of impurities have been considered ranging from the group I impurity K, to the group VI impurity Se. Notice that the bandgap is relatively "clean" of deep levels except for Zn, As and Se. Also notice that the T_C-site impurities have levels lower in energy than the T_A-site impurities. These calculations help us to understand why interstitial impurities are not energetically favored in III-V materials, but may be more energetically favorable in II-VI materials. They also show why the chemical potential is quite important in determining the energy of such defects since some defects have a number of charge states.

(b) Bandgap energy levels for the native interstitial impurities Zn and Se in ZnSe at the T_A and T_C interstitial sites.

Fig. 5.

Relaxation angle Θ as a function of time at the (110) surface for twelve semiconductors using a fictitious damping to determine the final equilibrium configuration. The atoms were allowed to move according to Newton's laws, where the forces were determined by including changes in the microscopic electronic states via the Hellmann-Feynman theorem. The angle Θ is a one measure of the relaxation of the surface atoms from their bulk atomic posititons. The final relaxation angle is found to be nearly the same for all these materials ranging from about 25 to 30 degrees.

F.g 5.

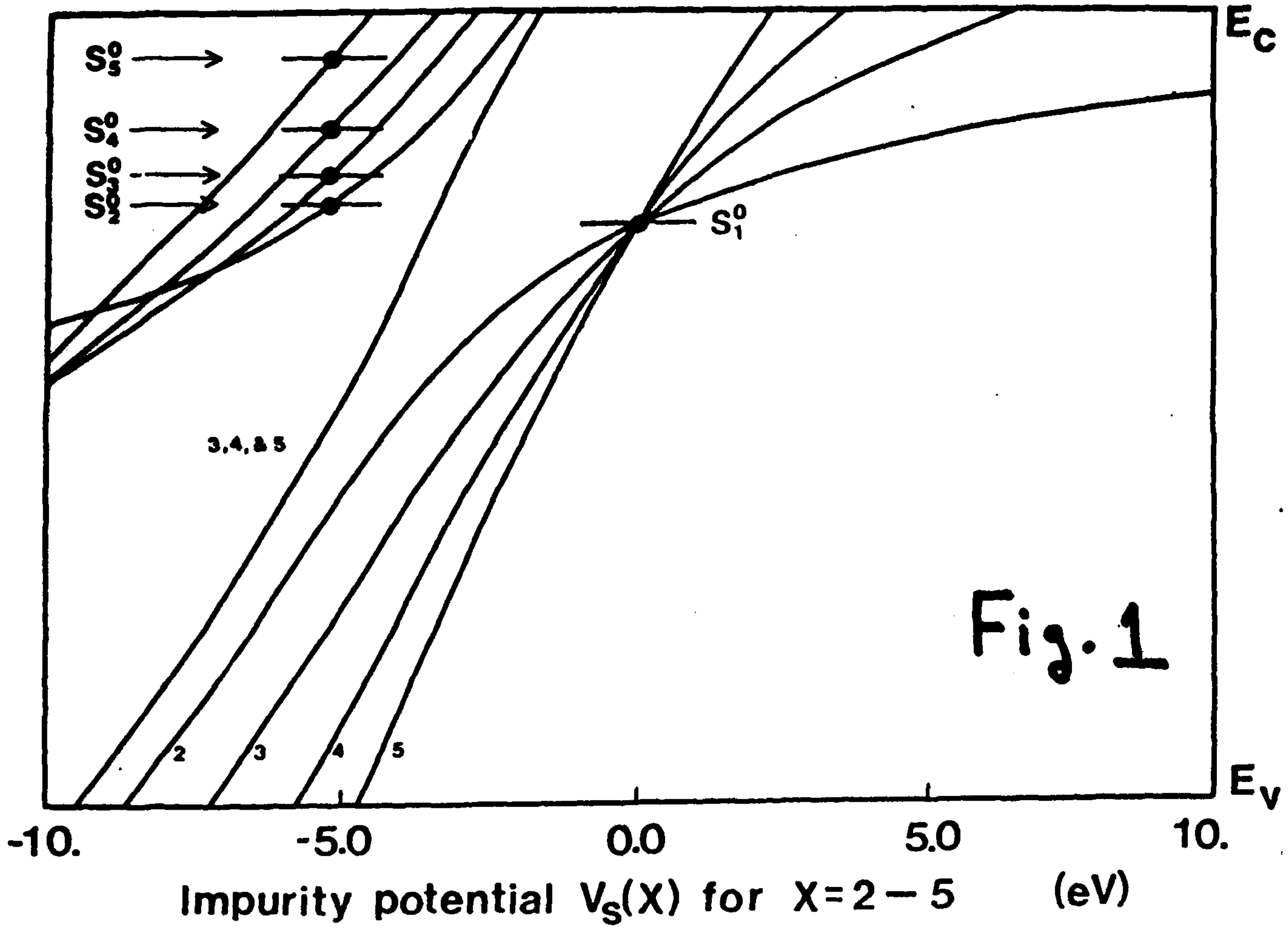
S_5^0
S_4^0
S_3^0
S_2^0
S_1^0
3,4, & 5
2
3
4
5
E_c
E_v
-10.
-5.0
0.0
5.0
10.
Impurity potential $V_S(X)$ for $X=2-5$ (eV)

Fig. 1

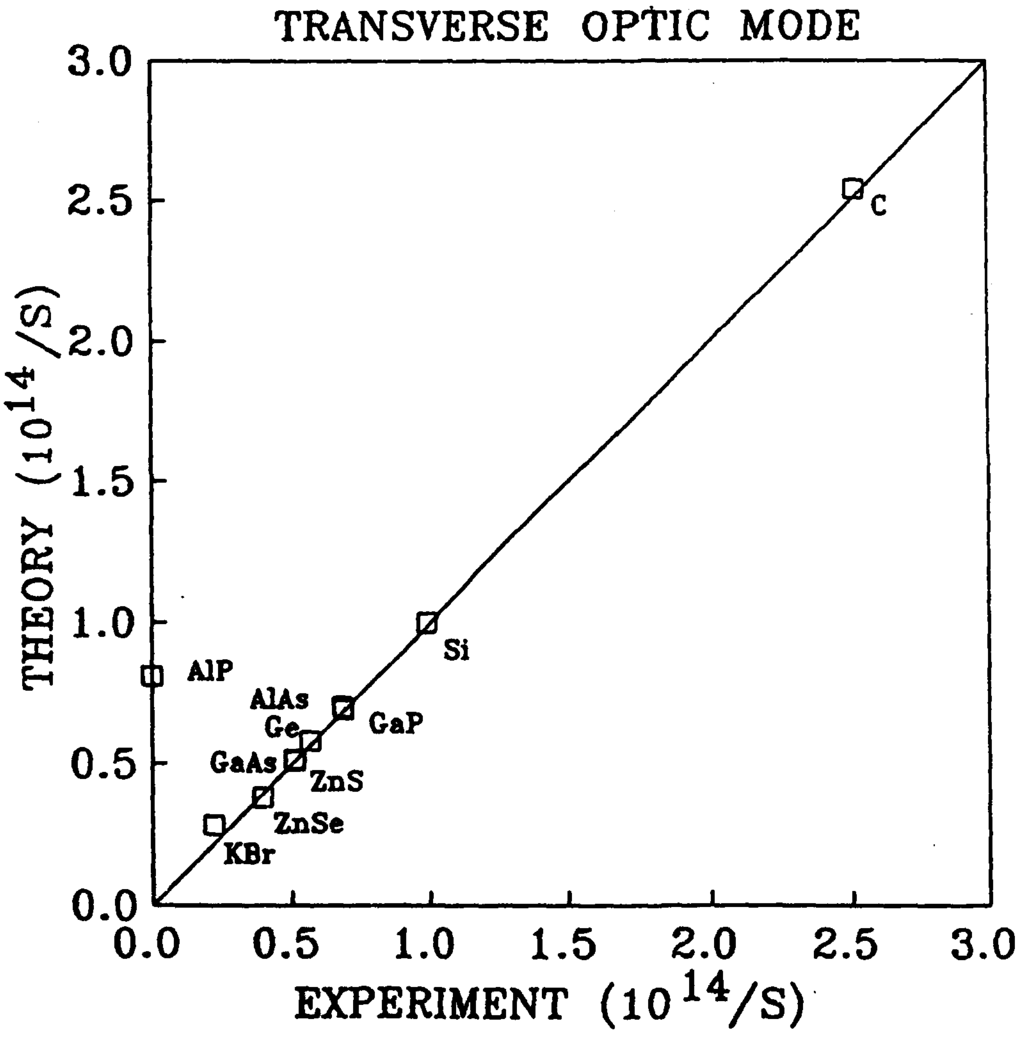
TRANSVERSE OPTIC MODE
THEORY (10^{14}/S)
EXPERIMENT (10^{14}/S)
0.0
0.5
1.0
1.5
2.0
2.5
3.0
C
Si
AlP
AlAs
Ge
GaP
GaAs
ZnS
ZnSe
KBr

Fig. 2a.

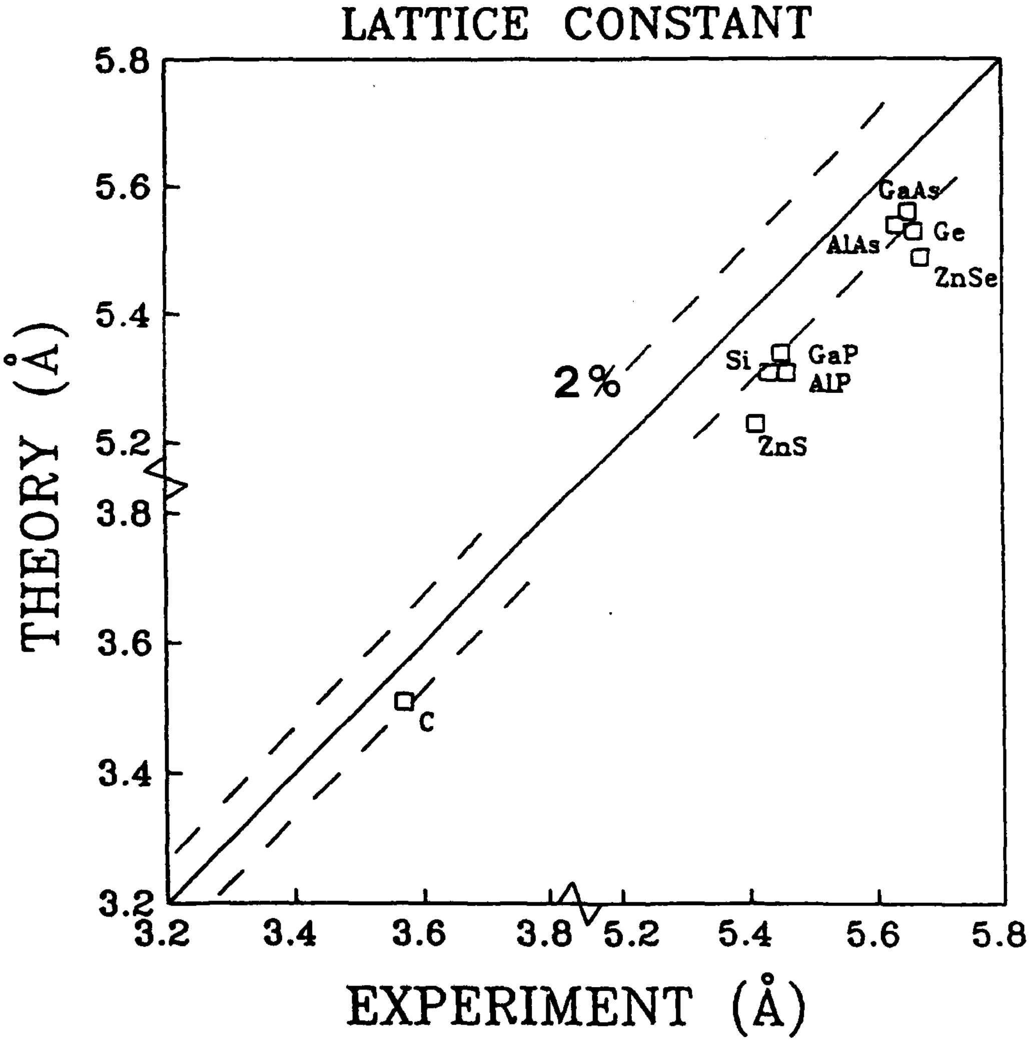
LATTICE CONSTANT
THEORY (Å)
EXPERIMENT (Å)
5.8
5.6
5.4
5.2
3.8
3.6
3.4
3.2
3.2
3.4
3.6
3.8
5.2
5.4
5.6
5.8
2%
GaAs
AlAs
Ge
ZnSe
Si
GaP
AlP
ZnS
C

Fig. 2b.

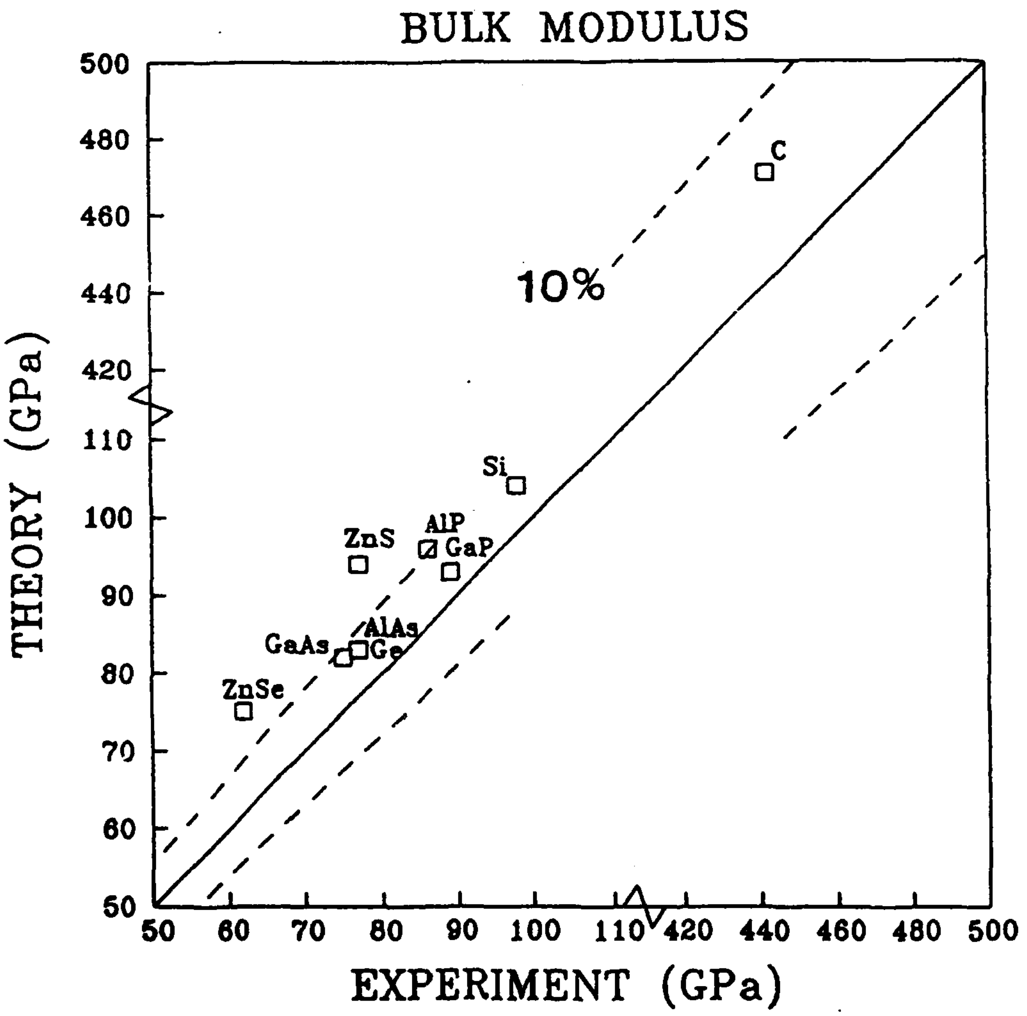
BULK MODULUS
THEORY (GPa)
EXPERIMENT (GPa)
500
480
460
440
420
110
100
90
80
70
60
50
50
60
70
80
90
100
110
420
440
460
480
500
10%
C
Si
AlP
GaP
ZnS
AlAs
GaAs
Ge
ZnSe

Fig 2c.

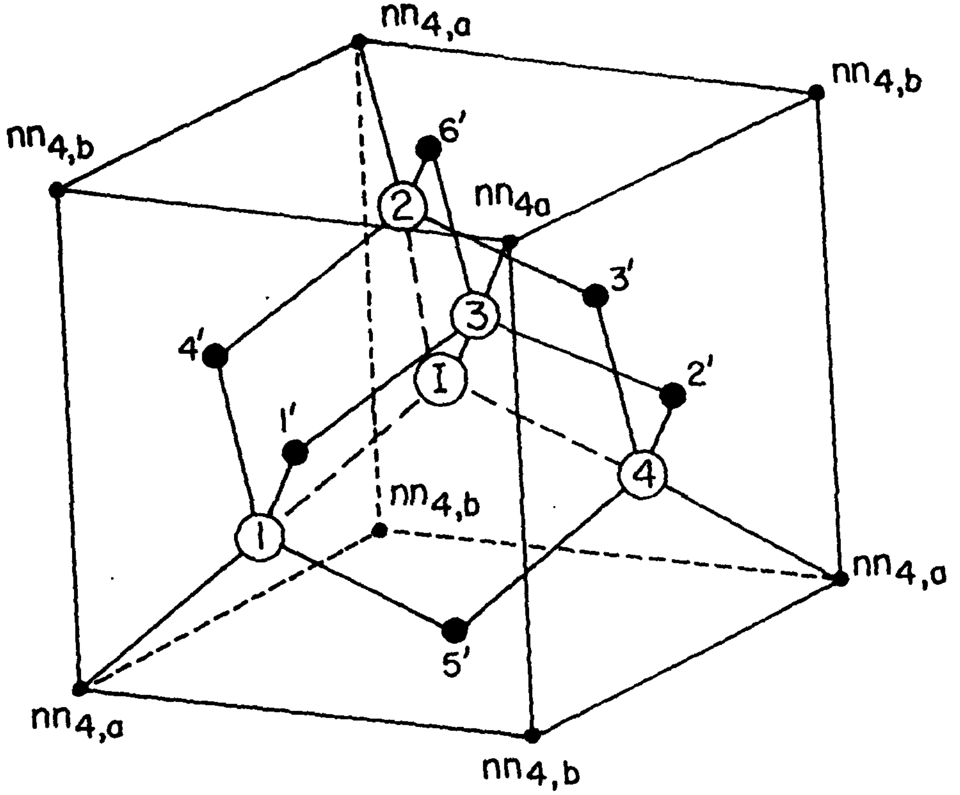

Fig.3a.

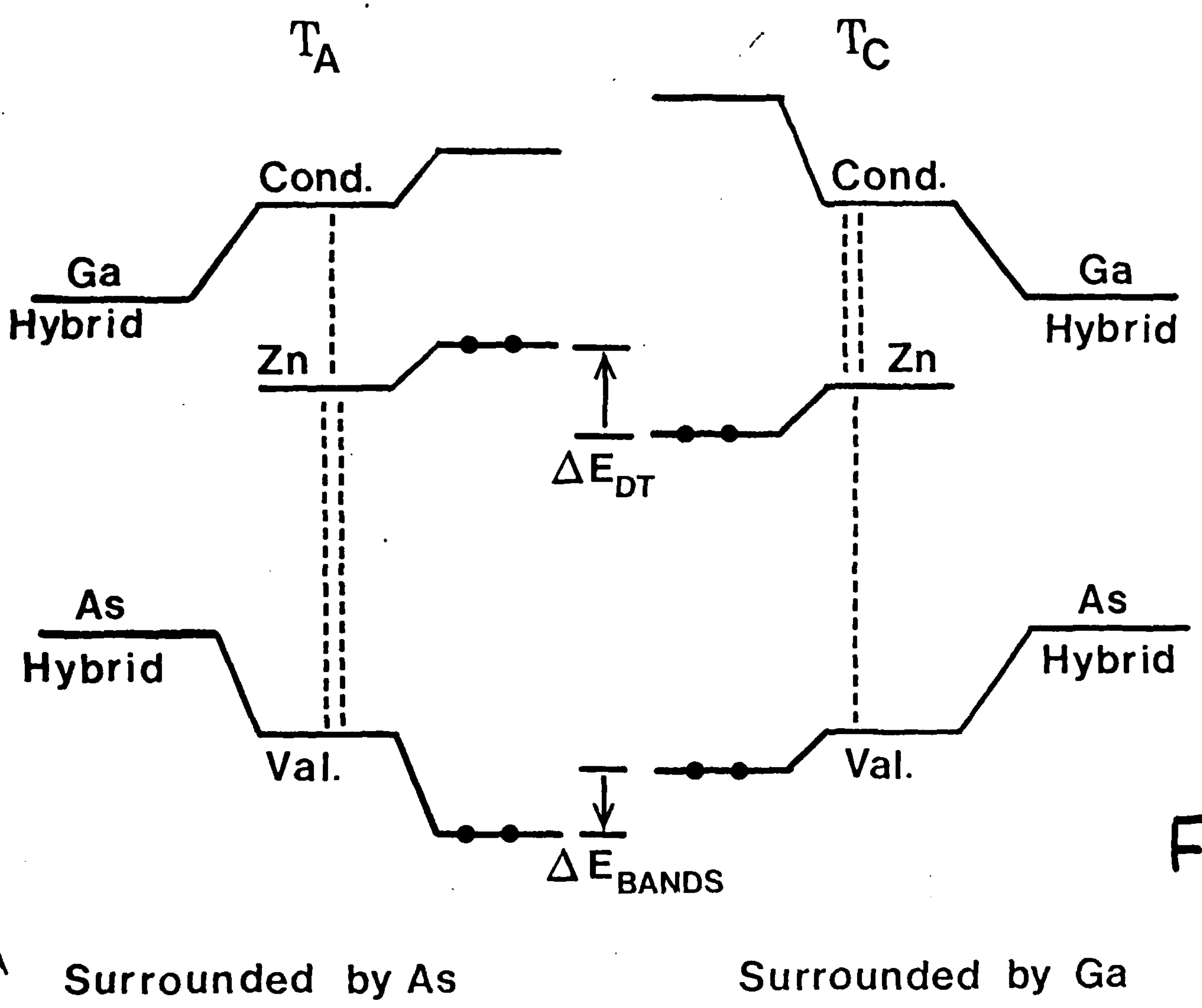
T_A
T_C
Cond.
Cond.
Ga Hybrid
Ga Hybrid
Zn
Zn
ΔE_{DT}
As Hybrid
As Hybrid
Val.
Val.
ΔE_{BANDS}
Surrounded by As
Surrounded by Ga

Fig 3b

Fig. 5

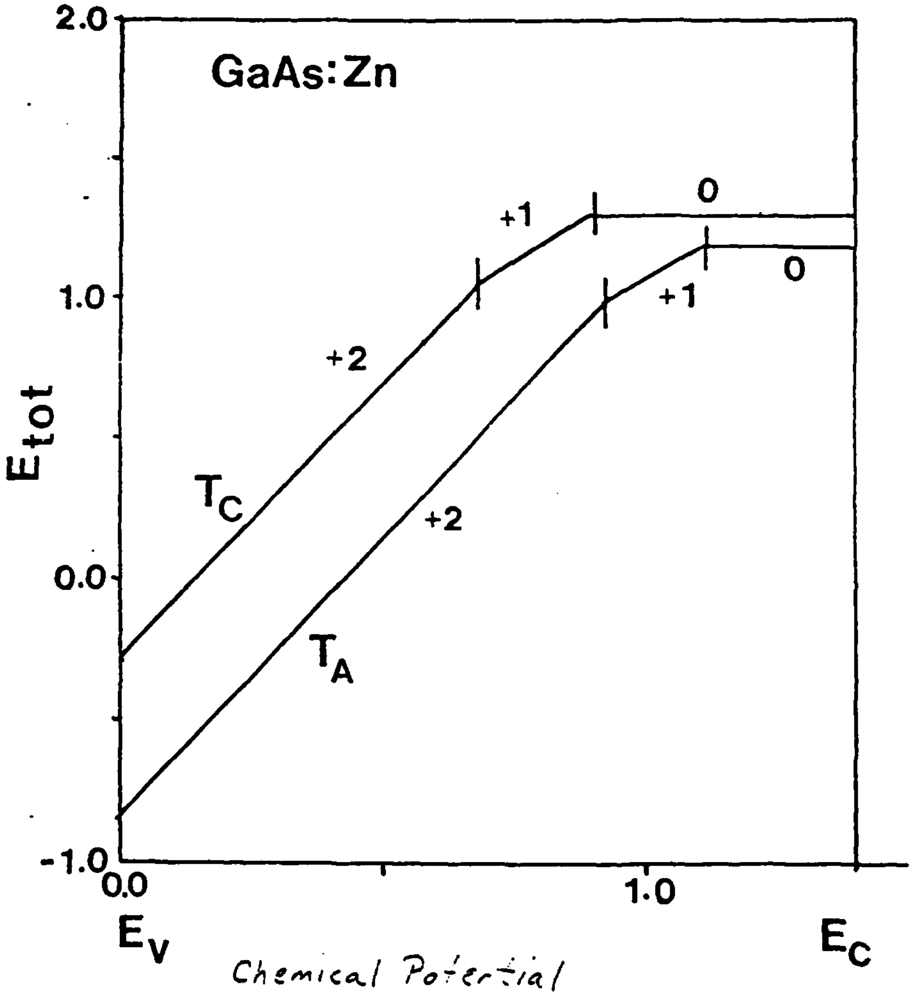
GaAs:Zn
2.0
1.0
0.0
-1.0
0.0
1.0
E_tot
E_V
E_C
Chemical Potential
T_C
T_A
+2
+1
0
+2
+1
0

Fig. 3c.

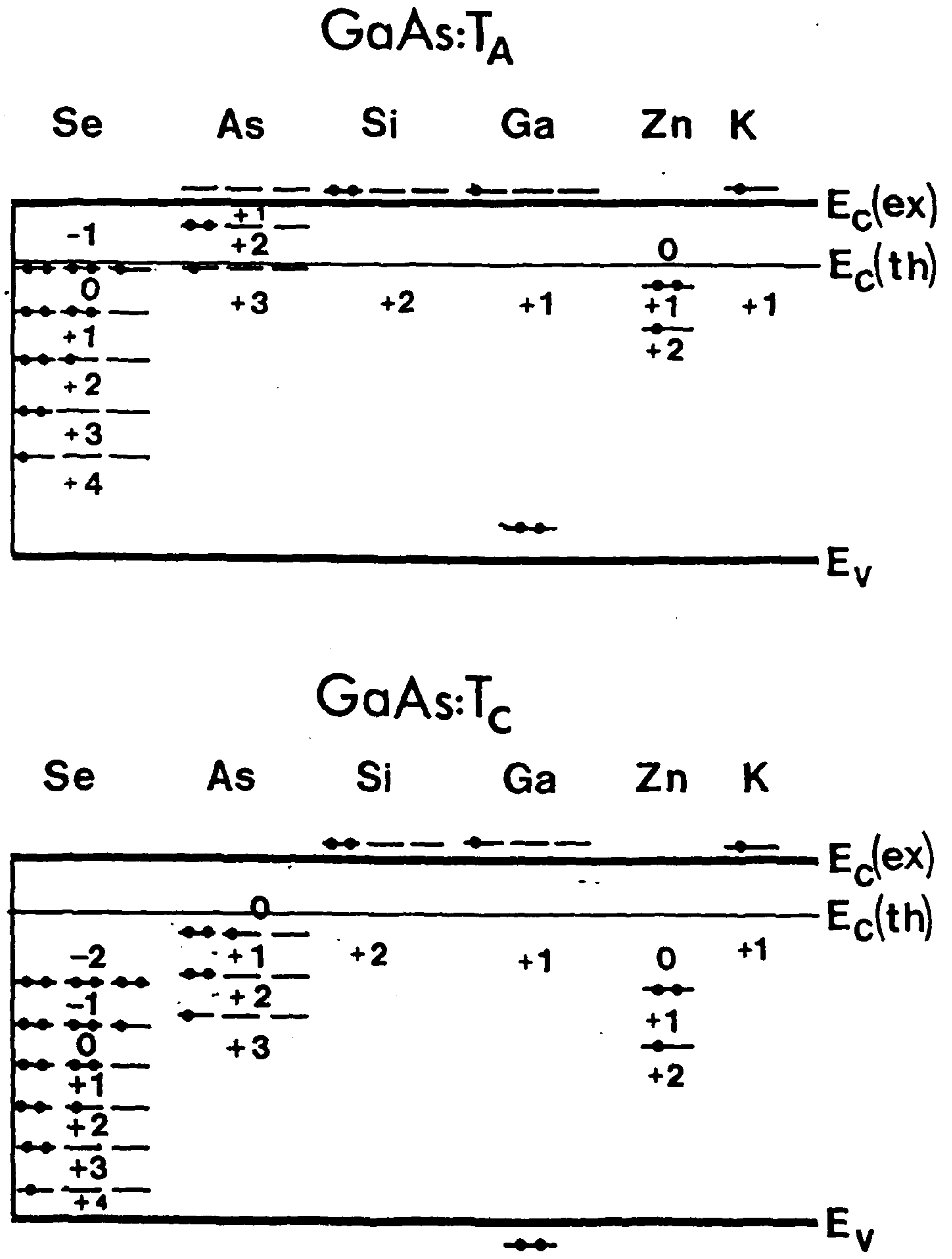

GaAs:T_A
Se
As
Si
Ga
Zn
K
E_c(ex)
E_c(th)
E_v
-1
0
+1
+2
+3
+4
+1
+2
+3
+2
+1
0
+1
+2
+1
GaAs:T_C
Se
As
Si
Ga
Zn
K
E_c(ex)
E_c(th)
E_v
-2
-1
0
+1
+2
+3
+4
0
+1
+2
+3
+2
+1
0
+1
+2
+1

Fig 4a.

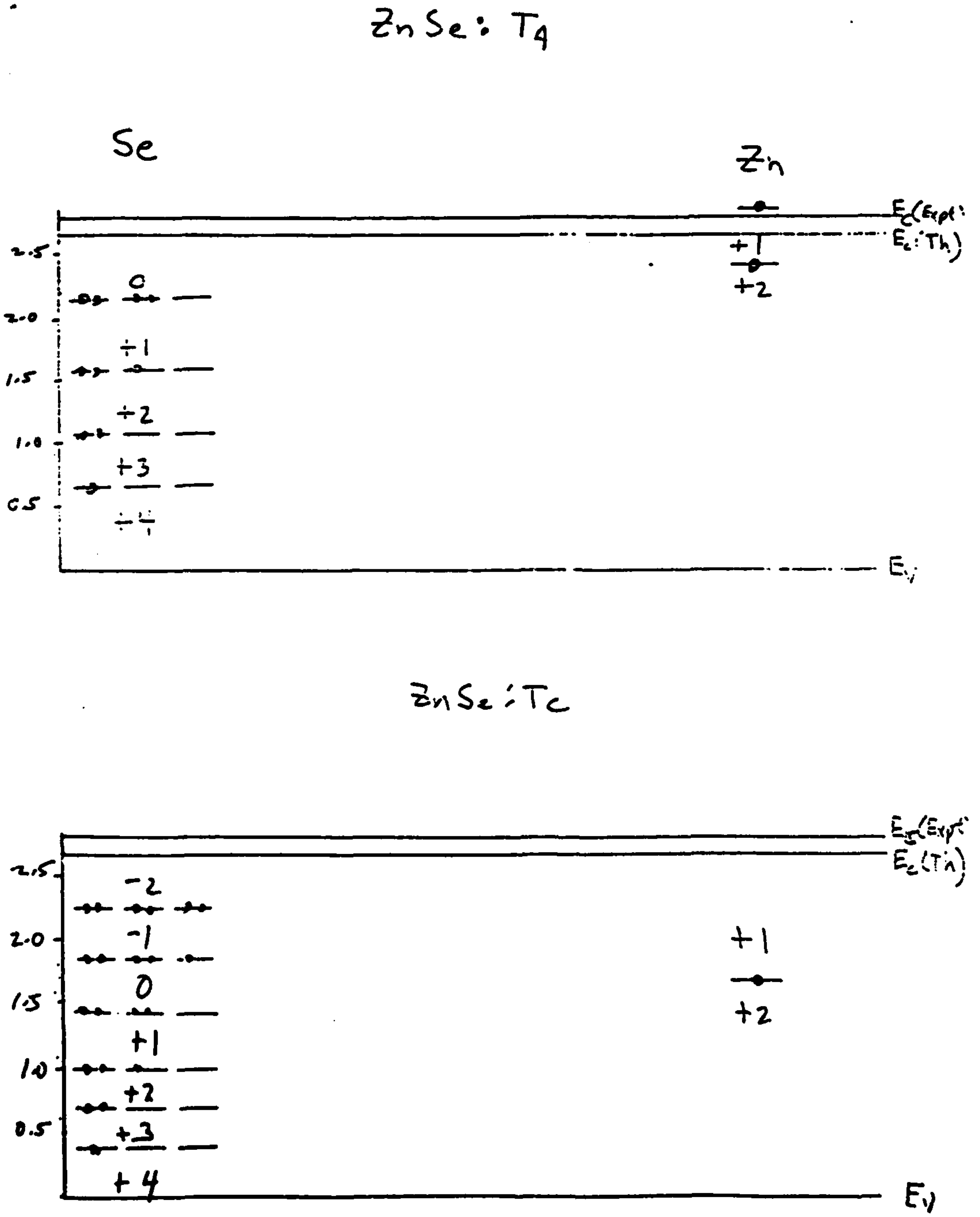
ZnSe: Td

ZnSe: Tc

Fig 4b.

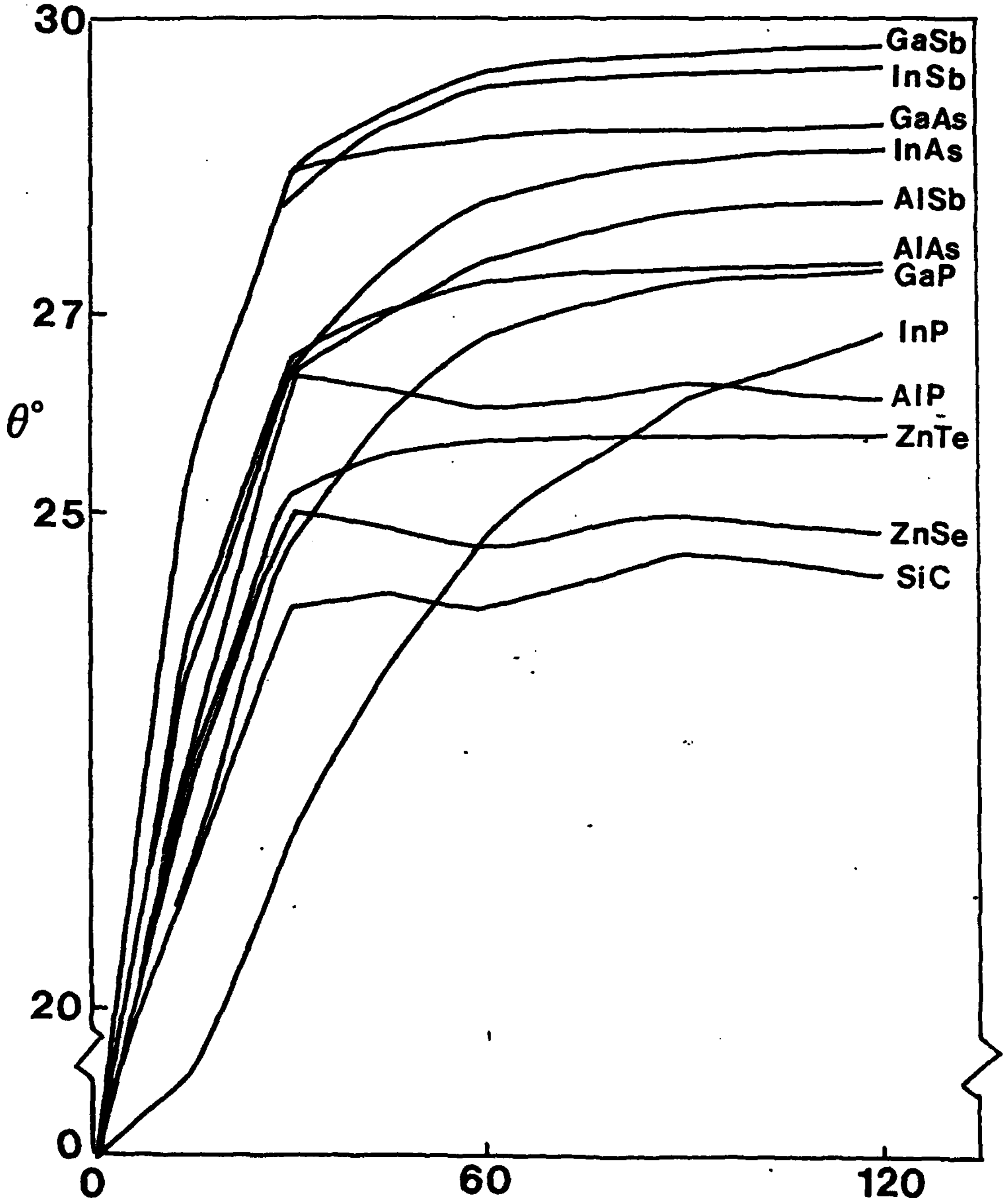
30
27
25
20
0
θ°
0
60
120
Time Step
GaSb
InSb
GaAs
InAs
AlSb
AlAs
GaP
InP
AlP
ZnTe
ZnSe
SiC

Fig. 5.

Fig. 5